**Olga V. Shapoval**

# SCIENTIFIC REPORT

on the exchange travel grant of the ESF Research and Networking Programme "Newfocus"
23 June - 11 September 2012
for the visit from the Institute of Radio-Physics and Electronics NASU, Kharkiv, Ukraine
to École Polytechnique Fédérale de Lausanne, Switzerland

## TOPIC: "RESONANCE EFFECTS IN THE TERAHERTZ ANTENNAS SHAPED AS FINITE COPLANAR GRAPHENE GRATINGS"

### PURPOSE OF THE VISIT

By agreement with the hosts, my work goal was an accurate study of the scattering and absorption of THz waves of two alternative polarizations by finite gratings of periodically structured coplanar grapheme-strip gratings. The proposed Nystrom-type numerical analysis is based on the median-line integral equations obtained using with the generalized boundary conditions and also on the quadrature formulas of interpolation type. Proposed algorithm is numerically efficient and guarantees fast convergence and controlled accuracy of computations. It allows to simulate fairly rapidly the scatterers consisting even of hundreds of microsize graphene strips. In particular, I planned investigate the interplay between the surface plasmon resonances dependent on each individual strip conductivity and width and the build-up of the Rayleigh anomalies at the wavelengths $\lambda = p/m,\ m = 1,2,...$ caused only by the periodicity and dependent on the number of strips in the grating.

### DESCRIPTION OF THE WORK CARRIED OUT DURING THE VISIT

During my visit from 23rd of June to 11st September 2012 I have:

- got understanding, from my hosts, of the electromagnetic properties of graphene layers in THz frequencies,
- investigated plane wave scattering and absorption by the coplanar graphene-strip grating in the THz range;
- studied the surface plasmon resonances emergence on the finite periodic grapheme-strip gratings in THz frequency range in the case of H-polarization and a gradual build-up of the Rayleigh anomalies as the strip number gets larger at the wavelengths $\lambda = p/m$, $m = 1,2$ in both H- and E-polarizations, but with more pronounced properties in the E-wave scattering ;
- investigated the tunability effects of the plasmon resonances of graphene strip gratings depending on the graphene chemical potential and relaxation time;
- analyzed gap size effects of finite periodic graphene-strip gratings;
- compared the plasmon nature of the finite and infinite free-standing graphene-strip gratings;
- presented results at the internal meeting of the Laboratory of Electromagnetics and Acoustics, EPFL;
- wrote a paper draft for IEEE Transactions on THz Science and Technology journal (to be submitted in 2012) and will prepare a joint conference paper for the 2013 URSI-B Symposium on EM Theory in Hiroshima.

The exchange visit gave me opportunity to study new area of application of my on-going studies into the resonant scattering and absorption of electromagnetic waves by thin-strip gratings – graphene strips in THz range. This was thanks to the expertise and collaboration of my hosts at LEMA-EPFL: Profs. J. Mosig and J. Perruisseau-Carrier and Dr. J.S. Gomez-Diaz. I hope that my stay and my work on the project will lead to more permanent research interaction between my home R&D laboratory and host laboratory at EPFL.

### DESCRIPTION OF THE MAIN RESULTS OBTAINED DURING THE VISIT

#### Problem formulation

The two-dimensional scattering and absorption of the H-polarized (vector $\vec{E}$ is across the strips) plane wave by finite periodic grating made of $N$ coplanar graphene strips is considered in THz frequency range. The corresponding free-standing geometry and the problem notations are shown in Fig. 1.

We suppose that the electromagnetic field is time-harmonic $e^{-i\omega t}$. The strips are assumed to be identical with the width $d$ and zero thickness, and are characterized with complex graphene conductivity $\sigma(\omega, \mu_c, \Gamma, T)$ calculated via the Kubo formulas [for

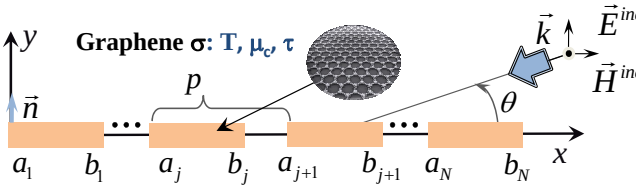


Fig. 1. Cross-section in the *XOY* plane of the studied free-standing finite periodic grating of $N$ infinitely long (lengthwise *OZ* axis) graphene strips of the same width $d$ and period $p$.

details see below] where $\omega$ is the radian frequency, $\mu_c$ is the chemical potential, $\tau$ is the relaxation time of charge carriers and $\Gamma = (2\tau)^{-1}$ is the phenomenological scattering rate that is assumed to be independent of energy, and T is the temperature.

As known, for a such 2-D problem one has to find a scalar function $H_z^{sc}(\vec{r})$ that is the scattered field *z*-component. In turn, the total field $H_z(\vec{r}) = H_z^{sc}(\vec{r}) + e^{-ik(x\cos\theta + y\sin\theta)}$, $\vec{r} = (x, y)$ must satisfy the Helmholtz equation off the strips' surface $S = \mathrm{U}_{j=1}^{N} S_j$, where $S_j = \{(x,0) : x \in [a_j, b_j]\}$, and $a_j$ and $b_j$ are the *j* strip endpoints. For the graphene sheets, the boundary conditions have been formulated relatively recently. It has been shown earlier that they take form of electrically-resistive sheet conditions which couple the tangential field components on the strips surface,

$$\partial[H_z^{+}(\vec{r}) + \vec{H}_z^{-}(\vec{r})] / \partial\vec{n} = -2ik(\sigma Z_0)^{-1}[H_z^{+}(\vec{r}) - \vec{H}_z^{-}(\vec{r})], \tag{1}$$

$$E_x^{+}(\vec{r}) = E_x^{-}(\vec{r}),\ \vec{r} \in S. \tag{2}$$

Here, *k* is free-space wa**ve**number and $Z_0 = (\mu_0 / \varepsilon_0)^{1/2}$ is free-space impedance and $\sigma$ is the graphene conductivity, and the indices ± correspond to the limit values of the field at the top and bottom sides of the strips.

**Nystrom-type discretization**

To satisfy Helmholtz equation and radiation condition, we seek the scattered field in the form of the *sum of* double-layer potentials,

$$H_z^{sc}(\vec{r}) = \sum_{j=1}^{N} \int_{S_j} w_j(\vec{r}\,') \frac{\partial G(\vec{r}, \vec{r}\,')}{\partial \vec{r}\,'} d\vec{r}\,', \tag{3}$$

where $G(\vec{r}, \vec{r}\,') = (i/4) H_0^{(1)}(k\,|\,\vec{r} - \vec{r}\,'\,|)$ is the Green function. Note that the unknown functions $w_j(\vec{r})$ are electric currents induced on the strips.

Using GBC (1)-(2) and the properties of the limit values of potentials in (3), we obtain a set of IEs of the second kind for $w_j(x^j)$, $j = 1, ..., N$ on the interval $x^j \in [a_j, b_j]$ with hyper-type singular kernel,

$$4(\sigma Z_0)^{-1} w_i(x_0^i) + \sum_{j=1}^{N} \int_{a_j}^{b_j} w_j(x^j) \frac{H_1^{(1)}(k\,|\,x^j - x_0^i\,|)}{|\,x^j - x_0^i\,|} dx = f(x_0^i), \tag{4}$$

where $f(x_0^i) = 4\sin\theta\, e^{-ikx_0^i\cos\theta}$, $x_0^i \in S_i$ $(i = 1, ..., N)$. Note the integral terms in (4) are understood in the sense of finite part of Hadamard, and corresponding currents $w_j(x^j)$ can be represented by means of new analytical functions $\tilde{w}_j(x^j)$: $w_j(x^j) = \tilde{w}_j(x^j)(x^j - a_j)^{-1/2}(b_j - x^j)^{-1/2}$ on interval $[a_j, b_j]$.

Further, we isolate the singularities of (4) in view of the asymptotic expansions for the Hankel functions,

$$\frac{H_1^{(1)}(k\,|\,x - x_0\,|)}{|\,x - x_0\,|} \sim ik\frac{\ln|\,x - x_0\,|}{\pi} - \frac{2}{\pi k\,|\,x - x_0\,|^2},\ x \to x_0 \tag{5}$$

and discretize resulted sets of IEs using Nystrom-type method based on the Gauss-Chebyshev quadrature formulas of interpolation type of the $n_w$-th order (with weight $\sqrt{1-t^2}$, $t \in (-1,1)$). As the discretization and collocations nodes we choose Chebyshev nulls $t_0^i = \cos(\pi i / (n_w + 1))$ of the second type. As a result, we derive independent $Nn_w \times Nn_w$ block-type matrix equations for the values of $w_j(t_0^i)$. On solving them numerically we obtain approximate solutions of IEs in the form of interpolations polynomials for the unknown surface currents. Then the field (3) can be easily reconstructed in the near and far zone of the strip grating.

The presented numerical algorithm is efficient and reliable and has theoretically guaranteed convergence (at least as $O(1/n_w)$) and controlled accuracy of computations.

**Graphene conductivity**

Graphene conductivity is characterized applying the Kubo formula,

$$\sigma(\omega, \mu_c, \Gamma, T) = jq_e^2(\omega - j2T)(\pi\hbar^2)^{-1}[(\omega - j2\Gamma)^{-1}\int_0^{\infty} \varepsilon\left(\frac{\partial f_d(\varepsilon)}{\partial\varepsilon} - \frac{\partial f_d(-\varepsilon)}{\partial\varepsilon}\right)\partial\varepsilon - \int_0^{\infty} \frac{f_d(-\varepsilon) - f_d(\varepsilon)}{(\omega - j2\Gamma)^2 - 4)(\varepsilon/\hbar)^2}\partial\varepsilon] \tag{6}$$

where the first term is related to interband contributions of graphene, which usually dominate in the low THz range, and the second term is related to interband contributions of graphene, which become more important at higher frequencies.

From the engineering point of view, it is useful to study the surface impedance of graphene defined as $Z_s = 1/\sigma$.

Fig. 2 shows the real and imaginary part of this quantity versus different values of the chemical potential, considering the temperature of T = 300 K and the relaxation time τ = 1 ps. Note that $\mu_c$ can be easily varied applying an external electrostatic field.

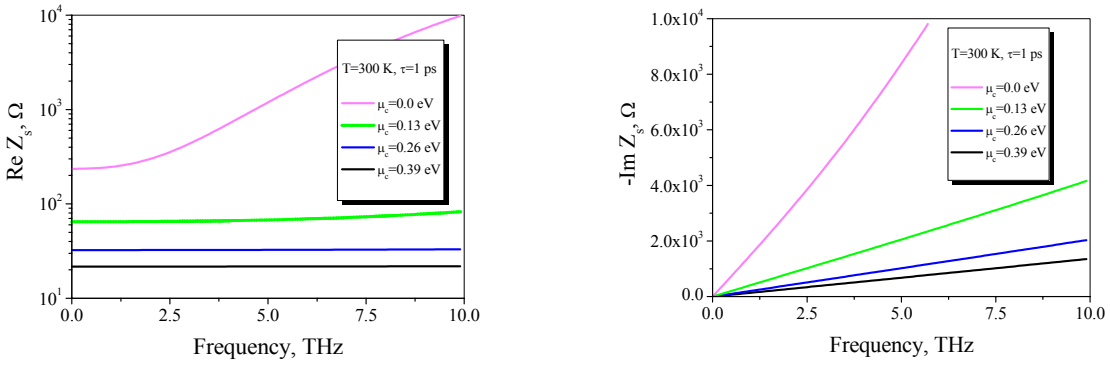


(a) (b)

Fig. 2. Real (a) and imaginary (b) parts of the surface impedance of graphene $Z_s = 1/\sigma$ in THz range calculated at the room temperature T = 300 K and $\tau$ =1 ps versus the chemical potential $\mu_c$.

Results show that graphene behaves almost as a frequency-independent resistor, with a purely inductive reactance. It is observed that an increase of the chemical potential $\mu_c$ leads to lower losses and an up-shift of the frequencies where graphene presents large inductive behavior. This particular features makes this material appropriate for the propagation of surface plasmon polaritons, which are transverse magnetic (TM) waves traveling along the interface between graphene and dielectric.

## Numerical results and discussions

### *Nystrom-Type Algorithm Convergence*

For the demonstration the actual rate of convergence, we have computed the root-mean-square deviations $\varepsilon_w = |\theta_w^{n_w} / \theta_w^{2n_w} - 1|$ of the uniform norms of the surface current functions $\theta_w = \left(\sum_{j=1}^{N} \| \tilde{w}_j \|^2\right)^{1/2}$, where $\| \tilde{w}_j \|^2 = \int_{-1}^{1} | \tilde{w}_j(t) |^2 \sqrt{1-t^2}\, dt$, versus the discretization order $n_w$. These results are shown in Fig. 3.

The errors decrease rapidly confirming the fast rate of convergence and solution stability. Thereby proposed Nystrom method on the basis of the quadrature rule of interpolation type ensures algebraic convergence of the approximate solution to the accurate ones with increasing the interpolation orders. For instance, to achieve 4-digit accuracy in the analysis one can take $n_w$ = 55 in the range of up to 10 THz and strip width of 20 μm.

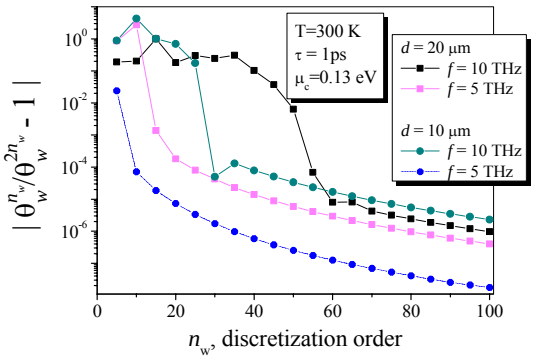


Fig. 3. The computation errors $\varepsilon_w$ as a function of the discretization orders $n_w$ for stand-alone graphene strip of different width $d$ = 10 and 20 μm at $f$ = 5 and 10 THz under the normal incidence of the H-wave

### *Stand-Alone Graphene Microsize Strip*

Stand-alone graphene microsize strips illuminated by the H-polarized wave in THz frequency range demonstrate a variety of surface plasmon resonances. In Fig. 4, the plots of TSCS (a) and ACS (b) as a function of the frequency are presented for the several stand-alone graphene strips of different width $d$ and different incidence angles, $\theta = \pi/2$ (solid curves) and $\theta = \pi/4$ (dotted curves), respectively.

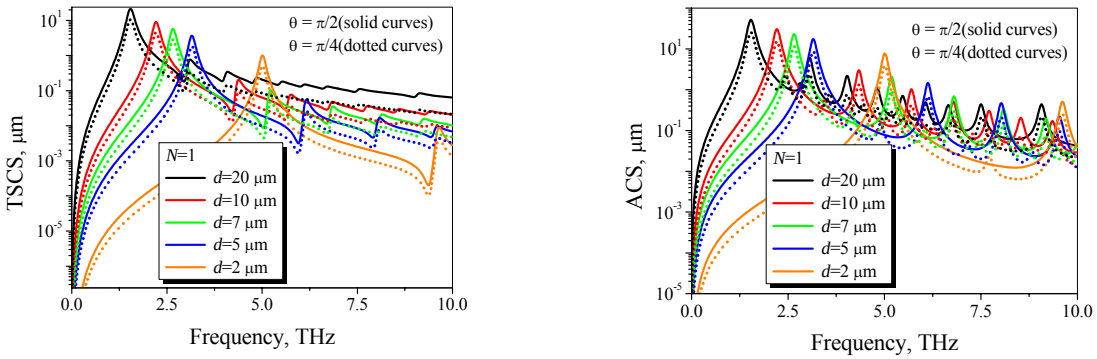


Fig. 4. TSCS (a) and ACS (b) versus the frequency in THz range for the normally (solid curves) and inclined (dotted curves) incident H-wave scattering by a stand-alone graphene strip of varying width *d*.

Here, the chemical potential is $\mu_c = 0.13\,\text{eV}$ and $\tau = 1\text{ps}$. Note the room temperature (T = 300 K) is assumed through the all calculation. As can be observed, the TSCS and ACS spectra variation depends on the strip width. The wider strips demonstrate larger number of resonating localized of surface plasmons in the considered THz range.
Figs. 5 (a)-(b) display the total near-field patterns at the first four plasmon resonances $H_n$, $n$ = 1,2,3,4 for the scattering by graphene strip of $d$ = 20 μm under the normal (a) and inclined (b) incidence, respectively.

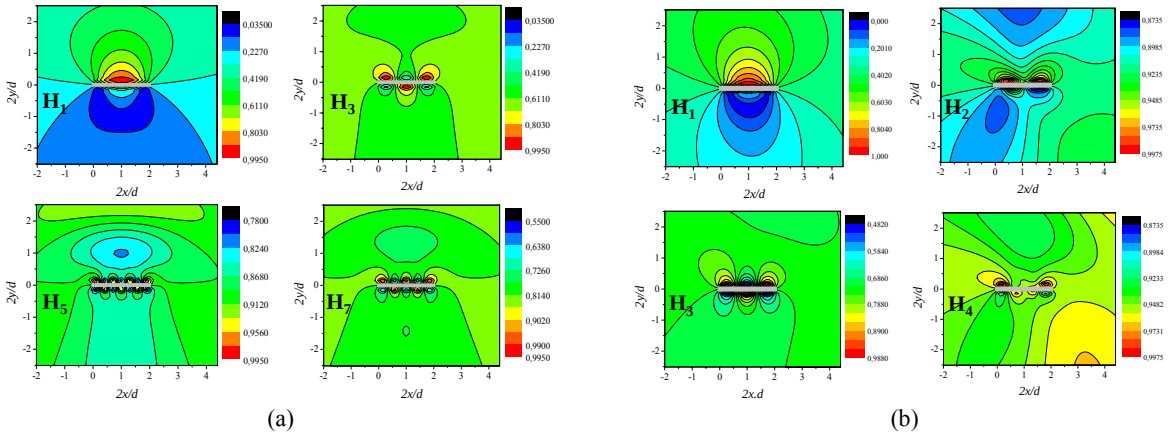


Fig. 5.Total near-field patterns for a stand-alone graphene strip under the normal (a) and inclined incidence (b) at four first resonances, $H_1$, $H_3$, $H_5$ and $H_7$ and $H_1$, $H_2$, $H_3$ and $H_4$, respectively.

As one can see, only odd-index resonances are excited at the normal incidence because of their symmetry across *y*-axis, and both odd and ever resonances are excited under the inclined incidence. Furthermore, we also investigated the spectral response of a free-standing graphene strip of width $d$ = 20 μm in dependence of the variation of the chemical potential $\mu_c$ and the relaxation time $\tau$.

Thereby, Fig. 6 shows that the surface plasmon resonances are quite sensitive with respect to the relaxation time changes. The associated peaks of TSCS and ACS became more pronounced if the τ increases.

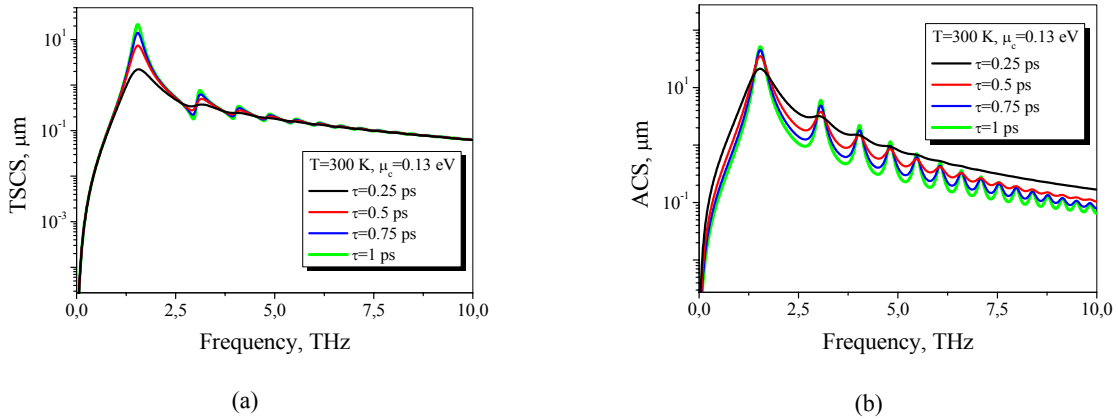


Fig. 6. TSCS (a) and ACS (b) versus the frequency in THz range for the normally incident H-wave light scattering by stand-alone graphene strip of width $d$ = 20 μm for the different values of the relaxation time $\tau$ =0.25, 0.5, 0.75 and 1 ps and fixed chemical potential $\mu_c$ = 0.13 eV

In its turn, the increasing of chemical potential with a fixed relaxation time $\tau = 1$ ps leads to the resistance decreasing (see Fig. 2 (a)) and results to the smaller number of the PRs within the considered frequency range, but is accompanied by significant enhancement of the absorption effect.

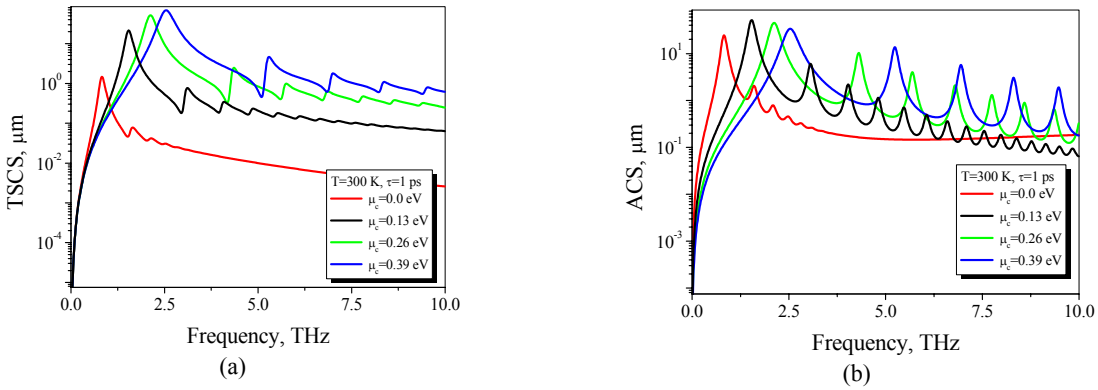


Fig. 7. TSCS (a) and ACS (b) versus the frequency in THz range for the normally incident H-wave scattering by a stand-alone graphene strip of the width $d = 20$ μm for the fixed relaxation time $\tau = 1$ ps and different values of the chemical potential $\mu_c$.

### *PR Prediction According to the Strip Width*

To obtain a better insight into the nature of PRs on the individual graphene microsize strips in free space, I have calculated the dependences of the resonant frequencies of 1st, 2nd, 3rd and 4th order plasmon resonance on the strip width (Fig. 8). As one can see, wider free-standing graphene strips demonstrate more resonances in the considered THz range with the lowest of them shifted to the lower frequencies.

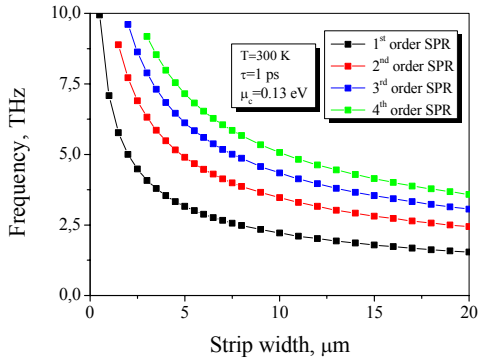


Fig. 8. Dependence of the frequency of 1st, 2nd, 3rd and 4th orders plasmon resonance on the graphene strip width.

### *Gap Size Effects of Finite Periodic Graphene Strip Gratings*

In Fig. 9, we present the plots of TSCS (a) and ACS (b) of the triple graphene strip grating of width $d = 20$ μm in the context of the gap size effects. As one can see, when the gaps between strips are large, e.g., $g = 30$ μm, the scattering and absorption spectra dictates only by the effects of the corresponding stand-alone strip.

In its turn, the nature of plasmon resonances on a triple strip gratings depends on the behavior of the stand-alone 60 μm of width strip and is accompanied by the slight shifting to the right with the increasing the gaps.

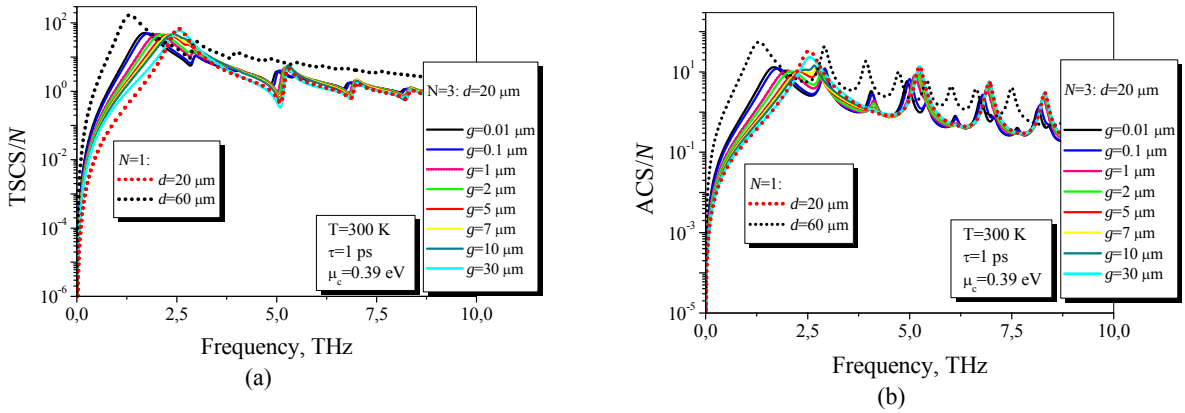


Fig. 9. Normalized TSCS (a) and ACS (b) versus the frequency in THz range for the normally incident H-wave scattering by grating of $N = 3$ strips of width $d = 20$ μm for the different values of gaps between strips $g$. Graphene conductivity parameters are T = 300 K, $\tau = 1$ ps and $\mu_c = 0.39$ eV

### *Comparison between H-wave and E-wave Scattering*

It is interesting to compare the scattering by infinite and finite gratings however it is far from obvious how to select a proper figure-of-merit. We have found that the efficiency of a finite strip grating of reflecting and transmitting a plane wave can be introduced as the part of TSCS associated with the power scattered into the upper and lower half-spaces, respectively, and normalized by the strip width $d$ and the number of strips $N$, and the absorbance is obtained directly

from the conservation of power. These quantities can be conveniently compared to the reflectivity, transmittance and absorbance of infinite grating normalized by the relative width subtended by a single strip.

Thereby, in Fig. 10 presented is such comparison of the H- and E-wave scattering by finite (e.g., $N$ = 10, 50) and infinite strip gratings of $d$ = 20 μm and $p$ = 70 μm. Note the alternative case of the E-polarized plane wave scattering (vector $\vec{E}$ is parallel to the strips), can be analyzed similarly using Nystrom-type discretization with Gauss-Legendre quadratures. As one can see, the H-polarization case demonstrates multiple plasmon resonances in THz range, and a gradual build-up of the Rayleigh anomalies at the associated wavelengths $\lambda = p/m$, $m = 1, 2$. In its turn, E-polarization case does not support any plasmon resonances, but demonstrate much more pronounced build-up of two Rayleigh anomalies: at the wavelength value equal to period $f_1 = 4.274 THz$ and at the twice smaller value $f_2 = 4.96 THz$.

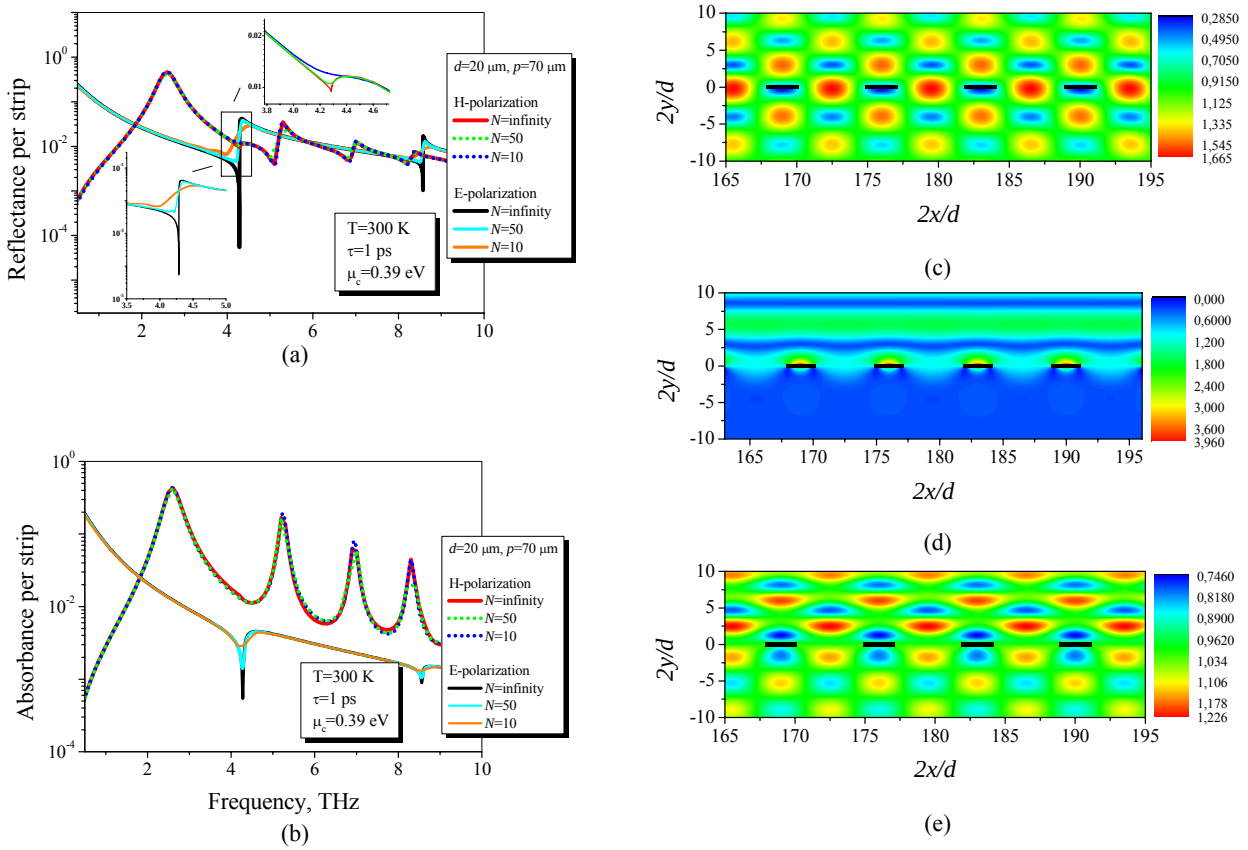


Fig. 10. Reflectance (a) and absorbance (b) for the normally incident H-wave and E-wave scattering by a grating of $N$ strips of $d$ = 20 μm and $p$ = 70 μm. Conductivity parameters are $\tau$ = 1 ps and $\mu_c$= 0.39 eV; and near E-field pattern around the strips ## 25 to 28 for the E-wave normally incident at the grating of $N$ = 50 graphene strips of $d$ = 20 μm and $p$ = 70 μm at Rayleigh anomaly frequency $f$ = 4.274 THz (c); and corresponding near H-field patterns for the H-wave scattering at the plasmon resonance $f$ = 2.6 THz (d) and at Rayleigh anomaly frequency $f$ = 2.27 THz (e).

As one can see, $N$ = 10 strips are enough to provide normalized reflectance and absorbance efficiency close to the infinite grating value in the whole band of frequencies from 0.1 to 10 THz, except for the narrow bands around the Rayleigh anomalies. In summary, we have presented numerically accurate analysis of the scattering and absorption of the plane waves by the finite and infinite periodic coplanar graphene strip gratings in the THz frequency range based on median-line singular integral equations Nystrom-type discretization. As an important side effect of our study, we have observed the high surface plasmon resonances localization of the finite periodic grapheme-strip gratings in THz frequency range in the case of H-polarization and a gradual build-up of the Rayleigh anomalies as the strip number gets larger at the associated wavelengths $\lambda = p/m$, $m = 1, 2$ in both cases of H- and E-polarization. Moreover, we have investigated the tunability of resonance effects on grapheme-strip gratings depending on the graphene chemical potential. It should be emphasized that, the graphene-strip gratings in comparison with the noble-metal strips, display pronounced surface-plasmon resonances in much lower frequency range, shifted to the THz wave.

**Planned publications based on the project work:**


1. O. V. Shapoval, J. S. Gomez-Diaz, J. Perruisseau-Carrier, J. R. Mosig and A. I. Nosich, "Plane wave scattering by coplanar graphene-strip gratings in the THz range," *IEEE Trans. THz Science and Techn.*, to be submitted in 2012.
2. O. V. Shapoval, J. S. Gomez-Diaz, J. Perruisseau-Carrier, J. R. Mosig and A. I. Nosich, "Plasmon resonances on graphene-strip gratings on THz frequencies," *Proc. URSI-B Symp. Electromagnetic Theory*, to be submitted in 2012.